AAS 20-462

MOON-TO-MOON TRANSFER METHODOLOGY FOR MULTI-MOON SYSTEMS IN THE COUPLED SPATIAL CIRCULAR RESTRICTED THREE-BODY PROBLEM

David Canales[*], Kathleen C. Howell[†], and Elena Fantino[‡]

Given the interest in future space missions devoted to the exploration of key moons in the Solar System and that may involve libration point orbits, an efficient design strategy for transfers between moons is introduced that leverages the dynamics in these multi-body systems. A general methodology for transfer design between the moons in any given system is developed within the context of the circular restricted three-body problem, useful regardless of the orbital planes in which the moons reside. A simplified model enables analytical constraints to determine the feasibility of a transfer between two different moons moving in the vicinity of a common planet.

INTRODUCTION

The exploration of planetary moons has always played a crucial role for an improved understanding of the Solar System and in the search for life beyond Earth. Past milestone missions to the gas giants incorporated tours of the moons and, thus, satisfied multiple science objectives at different targets simultaneously. For example, for the Galileo spacecraft, launched in 1989, engineers designed a 23-month tour in the Jovian system that was successfully accomplished[1] in the 1990s. Another well-designed tour was implemented for the Cassini-Huygens mission, launched in 1997, in the Saturn system,[2] demonstrating the advantage of tours for these types of missions in the 2000s. From these two missions, among others, scientific questions arise to be addressed in new mission proposals involving various worldwide space agencies. The ESA's JUICE mission,[3] for example, is proposed to study Ganymede, Callisto and Europa. The NASA missions include Europa Clipper[4] for the exploration of Europa, as well as Dragonfly,[5] whose goal is landing a robot on Titan.

To accomplish the design of increasingly complex mission scenarios requires effective trajectories with low propellant requirements, to support the construction of transfers between moons in a multi-body environment. One proposed strategy to tackle this problem is leveraging the coupled circular restricted three-body problem (coupled CR3BP) and locating connections between moons using Poincaré sections.[6–8] Generally, in such analyses, the identification of a suitable relative phase between the moons is not considered, and many studies assume that lunar orbits are coplanar. An alternative approach,[9–11] also a coplanar analysis, propagates departure and arrival trajectories to

[*]Ph.D. Student, School of Aeronautics and Astronautics, Purdue University, West Lafayette, IN 47907; dcanales@purdue.edu

[†]Hsu Lo Distinguished Professor of Aeronautics and Astronautics, School of Aeronautics and Astronautics, Purdue University, West Lafayette, IN 47907; howell@purdue.edu

[‡]Assistant Professor at Department of Aerospace Engineering, Khalifa University of Science and Technology, P.O. Box 127788, Abu Dhabi, United Arab Emirates; elena.fantino@ku.ac.ae

a certain distance from the moons, evaluates the osculating elements to represent these trajectories as conic arcs and determines any available tangential connections, producing an optimal relative phase between the moons as well as an analytically minimum-Δv option. However, despite having evaluated the error of the conic approximation[9] in the CR3BP, the result is not yet validated with a higher-fidelity model such as the coupled CR3BP or an ephemeris model. Of course, Lambert arcs[12] also offer the potential to identify the connection between invariant manifolds for two bodies moving around a common body.

Numerous previous investigations also involve gravity assists in multi-moon systems; strategies to exploit the moon gravity are examined via Tisserand graphs in the two-body problem (2BP),[13,14] the CR3BP[15] or a 2BP-CR3BP patched model.[16,17] Most preliminary studies using this technique include the assumption that the moons are in coplanar orbits. Such an approach reduces the Δv for maneuvers, but the transfer time of flight (t_{tot}) is sometimes considerably increased and the tour design process is computationally intensive. Although all the moons can be eventually encountered, the moon tour design is also challenging for other complex mission scenarios, e.g., leveraging libration point orbits, captures or even returning to a previously visited moon, since the gravity assists sequence is affected.

The focus of the present investigation is an alternative methodology for transfer design between moons for any given system; in particular, the use of dynamical structures in the three-body problem is examined. Using an analytical formulation from the spatial 2BP, this strategy enables construction of transfers in the coupled spatial CR3BP between moons in different planes. Also, for any transfer between moons where the analytical formulation holds valid, and for any given angle of departure from the departure moon, a potential transfer configuration is produced. As a result, additional insights are possible when designing tours. For example, potential new options may emerge throughout the course of the tour, such as transfers between different periodic orbits or alternatives for captures.

The dynamical models used for this investigation are first introduced. The analytical approach is then detailed to create a useful methodology for moon-to-moon transfers. Also, results are compared between a coplanar assumption for the moons orbits and moon motion modeled in terms of their actual inclined planes. A spatial application of the methodology is applied to transfers between Titania and Oberon. Finally, some concluding remarks are offered.

DYNAMICAL MODEL

When analyzing the motion in the vicinity of a moon, the CR3BP[18] is a simplified model that offers useful insight into trajectories and the general dynamical flow for many different applications. Designs constructed within such a framework are useful for preliminary analysis since they are usually straightforwardly transitioned to higher-fidelity ephemeris models.

For the purposes of this investigation, the CR3BP describes the motion of a spacecraft (s/c) subject to the gravitational force of a larger primary (planet) and a smaller primary (moon), both assumed to be in circular orbits about their common barycenter. In fact, most moons in the Solar System possess very small orbital eccentricities (e); the Earth-Moon system is characterized by one of the largest eccentricities at a value of 0.055. To model the problem, a system of differential equations in the CR3BP is written in dimensionless form such that the characteristic distance is the constant measure that defines the distance between the planet and the moon, and the characteristic time is selected to guarantee a dimensionless mean motion of the primaries equal to unity. The

mass ratio $\mu = m_{moon}/(m_{moon} + m_{planet})$ is defined as the characteristic mass parameter of the system, with m_{moon} and m_{planet} the masses of the moon and the planet, respectively. A rotating barycentric frame is defined with the $\hat{x}$-axis directed from the planet-moon barycenter to the moon, and the $\hat{z}$-axis from the barycenter in the direction of the angular momentum vector of the system. The planet and the moon are located at positions $\bar{r}_p = [-\mu, 0, 0]^T$ and $\bar{r}_m = [1-\mu, 0, 0]^T$, respectively. Note that overbars denote vectors whereas the subscript 'T' indicates the transpose of a vector. The evolution of the s/c position $\bar{r}_{rot} = [x, y, z]^T$ and velocity $\dot{\bar{r}}_{rot} = [\dot{x}, \dot{y}, \dot{z}]^T$ is defined by the following equations of motion:

$$\ddot{x} - 2\dot{y} = \frac{\delta U^*}{\delta x} \quad \ddot{y} + 2\dot{x} = \frac{\delta U^*}{\delta y} \quad \ddot{z} = \frac{\delta U^*}{\delta z}, \tag{1}$$

where dots are derivatives with respect to dimensionless time. All vectors are expressed in rotating coordinates. Then, $U^* = \frac{1-\mu}{r_{p-s/c}} + \frac{\mu}{r_{m-s/c}} + \frac{1}{2}(\dot{x} + \dot{y})$ represents the pseudo-potential function of the system of differential equations, and $r_{p-s/c}$ and $r_{m-s/c}$ are the distances between the planet and the s/c as well as the moon and the s/c, respectively. The Jacobi constant (JC) is defined as the "energy" of the s/c in the given system via $C = 2U^* - \sqrt{\dot{x}^2 + \dot{y}^2 + \dot{z}^2}$. Finally, note that motion exists in the vicinity of five equilibrium solutions in the given formulation. Such motion is frequently categorized by different types of families of periodic orbits according to their geometry and stability. Examples are the planar Lyapunov orbits family and the three-dimensional Halo orbits family. These orbits are leveraged for many different types of mission scenarios. Consistently with their stability properties, invariant manifolds that emanate from such periodic orbits often serve as pathways in the vicinity of the moons and to locate connections between periodic orbits within the same system.[19]

With one planet and two moons, each planet-moon system possesses its own characteristic quantities and angular velocities, and the moons' orbits are not located in the same plane. Given that the CR3BP only incorporates two bodies affecting the dynamics of the s/c, it is challenging to construct valid preliminary trajectories to travel from the vicinity of one moon to another using the CR3BP. Hence, it is useful to leverage some simplifications. The multi-body methodology for tour design is introduced using one sample scenario that involves a moon-to-moon transfer in the Jupiter's system; that is, trajectories departing from the vicinity of Ganymede and arriving in Europa's vicinity (see Table 1 for system's data). Since the orbital eccentricities of the two moons are small, Jupiter-Ganymede and Jupiter-Europa dynamics can be approximated with the CR3BP. The planes of the moon orbits are defined by the appropriate epoch in the Ecliptic J2000 frame, but the moons move in their respective circular orbit in their recognized orbital plane. The two models to tackle this problem are introduced below: (a) a two-body/three-body patched model (2BP-CR3BP patched model) and (b) a coupled three-body formulation.

Table 1. Orbital data of Europa and Ganymede (SPICE,[20] last accessed 08/05/2020).

	Semi-Major Axis [km]	Orbital Period [day]	μ [10^{-5}]	e	Inclination measured from Ecliptic J2000 [degree]	Right Ascension of the Ascending Node [degree]
Europa	$6.713 \cdot 10^5$	3.554	2.52802	0.00917	2.150	331.361
Ganymede	$10.706 \cdot 10^5$	7.158	7.80435	0.00254	2.208	340.274

2BP-CR3BP patched model

The 2BP-CR3BP patched model[9] approximates trajectories modeled in either the CR3BP or the 2BP depending on the location of the s/c in the system. Trajectories in the vicinity of a moon are modelled with the CR3BP. When these trajectories reach a certain distance from the moon, the motion is considered to be Keplerian with a focus at the larger primary and uniquely determined by the osculating orbital elements: semi-major axis (a) , eccentricity (e), right ascension of the ascending node (Ω), inclination (i), argument of periapsis (ω) and true anomaly (θ). For an example, Figure 1(a) illustrates one unstable manifold departing a Lyapunov orbit near the L_1 libration point in the Jupiter-Ganymede system. When the path reaches the sphere of influence (SoI) of the moon (see below), the state is transformed from the rotating frame to the Ecliptic J2000 Jupiter-centered inertial frame, and an osculating Keplerian orbit is obtained (Figure 1(b)). Similarly, trajectories arriving at the Europa vicinity are propagated backwards in time towards the SoI, where the state is instantaneously defined as a back-propagated Keplerian orbit in the inertial frame with Jupiter at its focus. Thus, both Jupiter-Ganymede (J-G) and Jupiter-Europa (J-E) systems are blended from their respective rotating frames into the Ecliptic J2000 Jupiter-centered inertial frame.

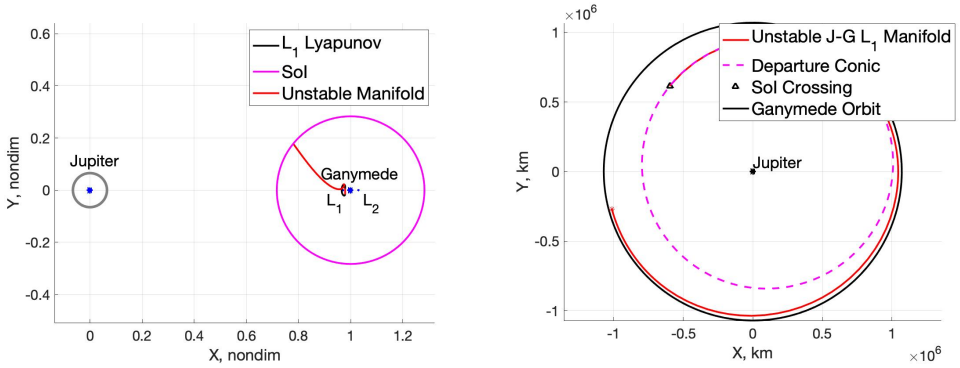

(a) Unstable manifold leaving the L_1 Lyapunov orbit in the Jupiter-Ganymede rotating frame. $JC = 3.0061$

(b) Departure conic after the manifold crosses Ganymede's SoI in the Ecliptic J2000 Jupiter-centered inertial frame.

Figure 1. Patched 2BP-CR3BP model for the Jupiter-Ganymede system.

The transformation of a state from the rotating frame to the Ecliptic J2000 Jupiter-centered inertial frame derives from a rotation that is easily determined with the following formulation. Assuming that the moons move on circular orbits defined in terms of an epoch using the Ecliptic J2000 frame, the position ($\bar{r}$) and velocity ($\dot{\bar{r}}$) of the s/c are obtained in the Ecliptic J2000 Jupiter-centered inertial frame given Ω_{moon}, i_{moon}, a_{moon} and θ_{moon}. Note that the moon location is evaluated using $\theta_{moon} = st + \theta_0$, where s is the angular velocity of the moon given the period in Table 1, t is the actual time in seconds, and θ_0 is the angle of the moon with respect to the ascending node line at the time of departure ($t = 0$). Given the moon's position ($\bar{r}_{moon}$) and velocity ($\dot{\bar{r}}_{moon}$) at a time t in the Ecliptic J2000 frame, employ $\bar{h}_{moon} = \frac{\bar{r}_{moon} \times \dot{\bar{r}}_{moon}}{|\bar{r}_{moon} \times \dot{\bar{r}}_{moon}|}$, i.e., the angular momentum of the moon at the given time along the trajectory. The rotation matrix is represented by $\mathbf{R} = [\hat{x}^T \ \hat{y}^T \ \hat{z}^T]$, such that $\hat{x} = \frac{\bar{r}_{moon}}{|\bar{r}_{moon}|}$, $\hat{z} = \frac{\bar{h}_{moon}}{|\bar{h}_{moon}|}$ and $\hat{y} = \frac{\hat{z} \times \hat{x}}{|\hat{z} \times \hat{x}|}$ define the axes of the planet-moon rotating frame at the given time. Note that boldface denotes a matrix. Given that the s/c rotating frame position and velocity states ($\bar{r}_{rot}$ and $\dot{\bar{r}}_{rot}$, respectively) are computed relative to the barycenter, μ is added to

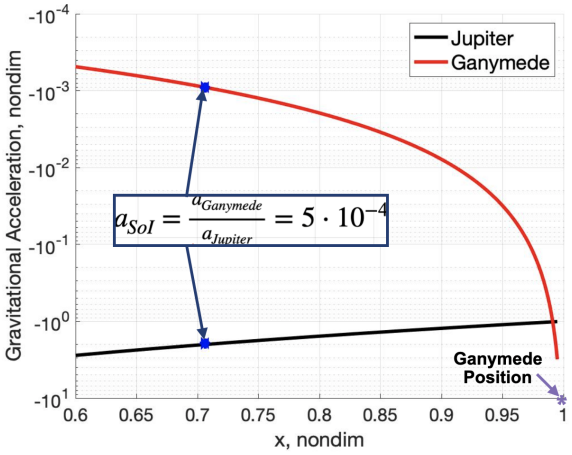

Figure 2. Gravitational acceleration variation due to Jupiter and Ganymede along the $\hat{x}$ axis.

the x-state of the position vector to shift the origin to the planet, but, the velocity components are the same after a translation. Using the basic kinematic equation, the velocity in the inertial frame, expressed in the rotating basis, is computed as $\dot{\bar{r}}_{in} = \dot{\bar{r}}_{rot} + \bar{s}_{rot} \times \bar{r}_{rot}$, being $\bar{s}_{rot} = [0\ 0\ s]^T$. As a result, the position and velocity in the inertial basis are defined by $\bar{r} = \mathbf{R}\bar{r}_{rot}$ and $\dot{\bar{r}} = \mathbf{R}\dot{\bar{r}}_{in}$.

The SoI is defined consistently with the variation in the gravitational acceleration of the planet and the moon along the $\hat{x}$ axis. An example for Jupiter and Ganymede of such a gravitational influence variation is provided in Figure 2. The radius of the SoI (R_{SoI}) is measured from the moon to the location where the gravitational acceleration ratio caused by the two primaries along the $\hat{x}$ axis corresponds to $a_{SoI} = \frac{a_{moon}}{a_{planet}} = 5 \cdot 10^{-4}$. Then, it is traced as a sphere surrounding the moon vicinity. The ratio value $a_{SoI} = 5 \cdot 10^{-4}$ is selected as the threshold since it is a sufficiently low moon gravitational acceleration for the motion of the s/c to be simplified to a planet-centered conic. If such a ratio is increased, the moon perturbation increases and the approximation may not be as valid. If the ratio is decreased, links between Jupiter-Ganymede and Jupiter-Europa trajectories might be missed and t_{tot} increases.

Coupled spatial CR3BP model

The coupled spatial CR3BP model considers trajectories from two different systems, each modeled in the CR3BP. For example, to design a trajectory from Ganymede to Europa, Jupiter-Ganymede and Jupiter-Europa CR3BP systems are overlapped at the common body, i.e., Jupiter. Assume that a transfer between Ganymede and Europa is the goal. Since the fundamental planes for both systems are different, use the following steps: CR3BP trajectories departing Ganymede are transformed from the rotating frame to the Ecliptic J2000 Jupiter-centered inertial frame; then, the resulting trajectory is rotated to the Jupiter-Europa rotating frame and a link between both trajectories is sought (Figure 3). In this frame, a Poincaré section at a certain angle with respect to the rotating Jupiter-Europa $\hat{x}$-axis is used to locate connecting trajectories between Ganymede and Europa.

The transformation of a state from the Ecliptic J2000 Jupiter-centered inertial frame to the rotating frame follows a reverse rotation. The rotation matrix is again defined by $\mathbf{R} = [\hat{x}^T\ \hat{y}^T\ \hat{z}^T]$, being $\hat{x} = \frac{\bar{r}_{moon}}{|\bar{r}_{moon}|}$, $\hat{z} = \frac{\bar{h}_{moon}}{|\bar{h}_{moon}|}$ and $\hat{y} = \frac{\hat{z}\times\hat{x}}{|\hat{z}\times\hat{x}|}$ the axes of the planet-moon rotating frame at the given time. Given the angular velocity of the moon in the inertial frame, $\bar{s}_{in} = \mathbf{R}\bar{s}_{rot}^T$, the state of the s/c in the rotating frame is expressed as $\bar{r}_{rot} = \mathbf{R}^T\bar{r}$ and $\dot{\bar{r}}_{rot} = \mathbf{R}^T(\dot{\bar{r}} - \bar{s}_{in} \times \bar{r})$. Finally, to locate the

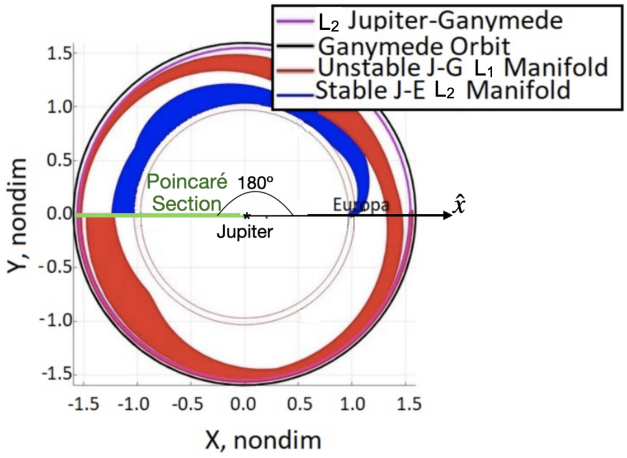

Figure 3. In red, unstable manifolds from L_1 Lyapunov orbit in the system ($JC_d = 3.0057$). In blue, stable manifolds from from L_2 Lyapunov orbit in the Jupiter-Europa system ($JC_a = 3.0028$). Poincaré section at 180°; Jupiter-Europa rotating frame.

state relative to the barycenter, μ is added to the x position component.

METHODOLOGY

Consider a s/c located in an L_1 Lyapunov orbit in the Jupiter-Ganymede system with a Jacobi Constant value $JC_d = 3.0061$. Let the target destination be an L_2 Lyapunov orbit ($JC_a = 3.0024$) in the Jupiter-Europa system. Unstable manifolds depart the L_1 Lyapunov orbit in the J-G system and stable manifolds arrive at the L_2 Lyapunov orbit in the J-E system. Determining the natural intersection between these manifolds presents a challenge. This methodology consists of first using the 2BP-CR3BP patched model to analytically explore promising trajectories and configurations between two different moons. Once a promising transfer is uncovered, such a transfer serves as an initial guess for the coupled spatial CR3BP. For the sake of comparison, the problem is explored assuming the orbits of the moons are coplanar and, then, in different planes. Note that the strategy applies for any moon-to-moon transfer with a common planet.

Moons on coplanar orbits

Analytical constraint for a successful transfer. Assume, for now, that the orbits of Ganymede and Europa are in the same plane. The 2BP-CR3BP patched model is used to construct analytical connections between trajectories in the different systems. Trajectories departing Ganymede's vicinity are propagated towards the Ganymede SoI and, when the s/c reaches it, a departure conic with orbital elements dependent on the initial Ganymede epoch angle $\theta_{0_{Gan}}$ is obtained. Desirable trajectories for arrival in Europa's vicinity are also back-propagated to the Europa SoI, where an arrival conic with orbital elements dependent on the Europa arrival epoch angle $\theta_{4_{Eur}}$ is produced. Recall that the subscript '4' is used to represent the arrival instant. The objective is the determination of the geometrical condition that both departure and arrival conics must possess for intersection.[21] Two confocal ellipses may have up to two point in common,[9] r_{int}, as long as

$$r_{int} = \frac{p_d}{1 + e_d \cos\theta_d} = \frac{p_a}{1 + e_a \cos\theta_a}, \tag{2}$$

where a_d and a_a are the semi-major axes, e_d and e_a are the eccentricities, θ_d and θ_a the true anomalies at the intersection of the departure and arrival conics, respectively, and $p_d = a_d(1 - e_d^2)$ and

$p_a = a_a(1 - e_a^2)$. The angle θ_a is defined as $\theta_a = \theta_d - \Delta\omega$, where $\Delta\omega = \omega_a - \omega_d$. Given the trigonometric property $\cos(\theta_d - \Delta\omega) = \cos\theta_d \cos\Delta\omega + \sin\theta_d \sin\Delta\omega$, the following expression is produced:

$$p_d - p_a + (p_d e_a \cos\Delta\omega - p_a e_d)\cos\theta_d = -p_d e_a \sin\Delta\omega \sin\theta_d. \tag{3}$$

Squaring both sides of Eq. (3) yields the quadratic equation $k_1 \cos^2\theta_1 + 2k_2 \cos\theta_1 + k_3 = 0$ with the following solution:

$$\cos\theta_d = \frac{-k_2 \pm \sqrt{k_2^2 - k_1 k_3}}{k_1}, \tag{4}$$

where $k_1 = (p_d e_a \cos\Delta\omega - p_a e_d)^2 + (-p_d e_a \sin\Delta\omega)^2$, $k_2 = (p_d - p_a)(p_d e_a \cos\Delta\omega - p_a e_d)$ and $k_3 = (p_d - p_a)^2 - (-p_d e_a \sin\Delta\omega)^2$. Looking into Eq. (4), only one solution is available when $k_2^2 - k_1 k_3 = 0$. This limiting case corresponds to a tangential intersection between the two conics (Figure 4). Trajectories that intersect tangentially frequently correspond to a theoretical minimum Δv,[9] certainly in terms of the minimum energy for each given maneuver. From $k_2^2 - k_1 k_3 = 0$, an ideal phase for the arrival moon is delivered such that a tangent configuration is guaranteed. The appropriate arrival conic reorientation for a tangent configuration is defined:

$$\cos\Delta\omega = \frac{2a_a a_d - a_a^2(1 - e_a^2) - a_d^2(1 - e_d^2)}{2a_a a_d e_a e_d}. \tag{5}$$

For computational implementation, focus on the right side of Equation (5). The inequality constraint $2a_d a_a(1 + e_d e_a) < b_d^2 + b_a^2$ is obtained when $\frac{2a_a a_d - a_a^2(1-e_a^2) - a_d^2(1-e_d^2)}{2a_a a_d e_a e_d} < -1$, where b_d and b_a are the semi-minor axis of the departure and arrival conics, respectively. This conditions implies that the departure and arrival conics never intersect. When both sides of the equation equate, the minimum condition for tangency is produced, which occurs between the apogee of the inner conic and the perigee of the outer conic. Furthermore, when $\frac{2a_a a_d - a_a^2(1-e_a^2) - a_d^2(1-e_d^2)}{2a_a a_d e_a e_d} > 1$, the inequality constraint yields $2a_d a_a(1 - e_d e_a) > b_d^2 + b_a^2$, that implies two intersections between the conics are available. Therefore, when both sides of the equation equate, the maximum limiting geometrical relationship between the ellipses emerges, one such that a tangent configuration occurs: an apogee-to-apogee or perigee-to-perigee configuration results, depending on the properties of both ellipses. Thus, the following geometrical constraints are produced:

$$2a_d a_a(1 + e_d e_a) \geq b_d^2 + b_a^2 \geq 2a_d a_a(1 - e_d e_a), \tag{6}$$

If the geometrical properties for two conics fulfill the inequality constraint represented in Eq. (6), they can be reoriented and tangentially connected.

Arrival moon's rephasing. Given an arrival conic that satisfies Eq. (6) and that is reoriented such that it intersects tangentially with a departure conic, it is possible to compute the angle at which the conic intersects the SoI: $\sigma = \omega_a + \theta_{SoI}$. Such an angle is projected onto the arrival moon plane, and is measured from its right ascension line in the Ecliptic J2000 frame; if the inclination of the arrival moon's plane is zero, it is measured from the x-axis in the Ecliptic J2000 Jupiter centered inertial frame (Figure 4). Let $\delta = \tan^{-1}(\frac{y_{SoI}}{|x_{SoI}|})$ be the angle between the intersection of the trajectory with the SoI and the $\hat{x}$ axis in the rotating frame. Then, the angle of the moon in its orbit at the end of the transfer, $\theta_{4_{Eur}}$, is evaluated:

$$\theta_{4_{Eur}} = \sigma - \delta + \frac{2\pi\Delta t_a}{P_{moon}}, \tag{7}$$

where Δt_a is the total time along the arrival CR3BP trajectory in the arrival moon vicinity, and P_{moon} is the period of the arrival moon in its orbit.[22]

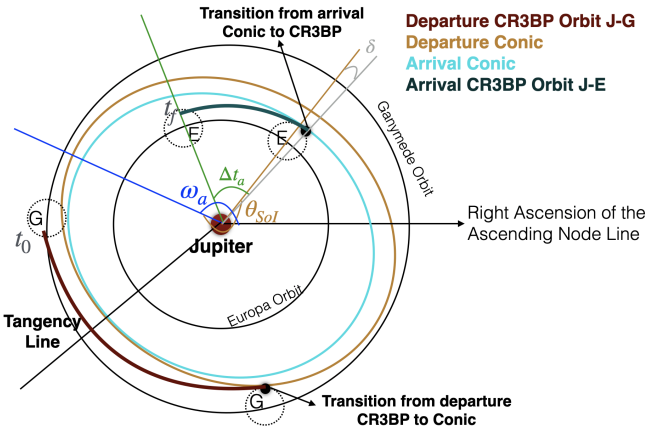

Figure 4. Representation of the rephasing of the arrival moon for a tangent configuration. All angles are measured projected upon the arrival moon plane.

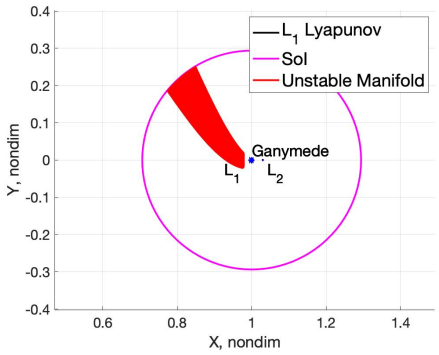

(a) L_1 Lyapunov orbit's unstable manifolds towards Ganymede SoI ($JC_d = 3.0061$). J-G rotating frame.

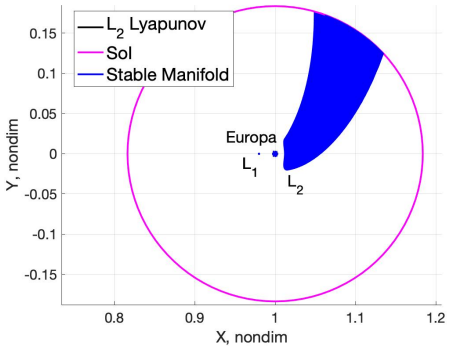

(b) L_2 Lyapunov orbit's stable manifolds towards Europa SoI ($JC_a = 3.0024$) J-E rotating frame.

Figure 5. Departure trajectories from the Ganymede vicinity (left) and arrival trajectories at the Europa vicinity (right).

Ganymede to Europa transfer. Unstable manifolds are propagated from the L_1 Lyapunov orbit in the J-G system towards Ganymede's SoI, where they transition into departure conics, similar to the stable manifolds arriving into the L_2 Lyapunov orbit in the J-E system from Europa's SoI, where they become arrival conics in backwards time (Figure 5). Then, it is possible to determine from the inequality constraint in Eq. (6) which trajectories intersect tangentially, as well as the total Δv for the maneuver at the intersection point after applying Eq. (5) (Figure 7(a)). The black line in Figure 7(a) separates the lower boundary reflecting the inequality constraint in Eq. (6) ; i.e., outside the colormap, all the departure conics are too large for any arrival conics to intersect tangentially. The angle in Figure 7(a) corresponds to the location of departure/arrival on the manifold along the periodic orbit, measured as reflected in Figure 6. The manifold trajectory leading to a tangential Δv connection between the moons is then constructed[9] (Figure 7). Since the orbits of the moons are coplanar, the total Δv, t_{tot} and the transfer configuration are constant regardless of the angle of departure $\theta_{0_{Gan}}$ (i.e., departure epoch in the Ganymede orbit).

Selection of the manifold corresponding to the minimum Δv in such a simplified model enables connections in the coupled CR3BP. To identify such links, the following angles are identified

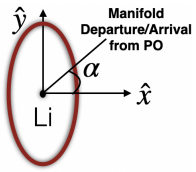

Figure 6. Angle of departure/arrival of the manifold from/to the periodic orbit.

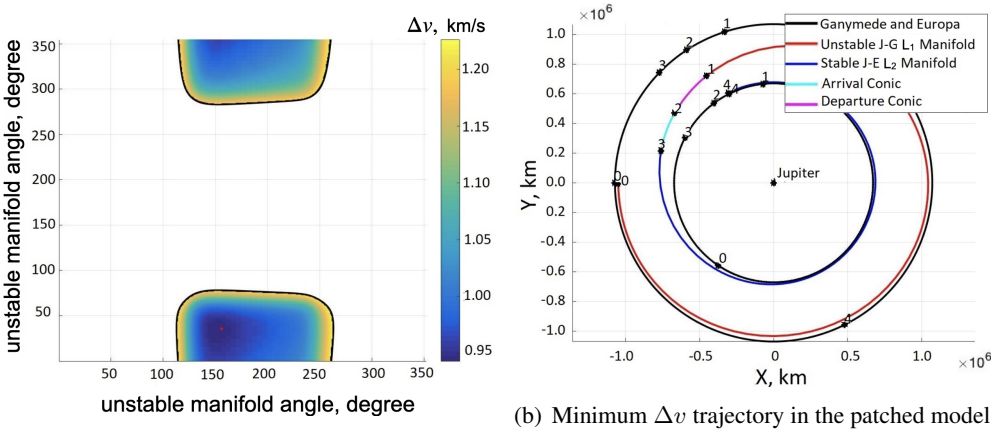

(a) All minimum Δv tangent configurations. Angle projected onto the x-y plane and measured counter-clockwise from the $\hat{x}$-axis of the rotating frame.

(b) Minimum Δv trajectory in the patched model CR3BP + 2BP in the Ecliptic J2000 Jupiter-centered inertial frame. $\Delta v = 0.9433$ km /s and $t_{tot} = 9.47$ days.

Figure 7. Transfer from unstable manifolds leaving from L_1 in the J-G vicinity ($JC_d = 3.0057$) to stable manifolds arriving to L_2 in the J-E vicinity ($JC_a = 3.0024$), assuming moons are coplanar.

from Figure 7(b): (a) the initial phase between the moons is computed measuring the location of Ganymede from the Europa location at instant 0 for both; (b) a time-of-flight is determined for both the unstable and stable manifolds at instant 2 (intersection between departure and arrival conics in Figure 7(b)). A final converged connection between the moons then appears in Figure 8. Furthermore, the resulting trajectory possesses a very similar t_{tot} and Δv as compared to the patched conic model. The initial guess from the simplified model is reasonably efficient as compared to analyzing all possible scenarios with Poincaré sections. Consequently, the 2BP-CR3BP patched model offers a good initial guess to construct a transfer in the planar coupled CR3BP problem. The importance of Eq. (6) is significant: that is, a necessary condition that must be fulfilled to locate tangential connections between planar trajectories linking two coupled CR3BP. Also, Eq. (6) can be leveraged as a constraint to produce feasible transfers in the CR3BP where the motion of the s/c is mainly governed by one primary and the trajectories are planar.

Moons on non-coplanar orbits

Analytical constraint for a successful transfer. The next level of complexity is a strategy to produce a successful transfer considering that both moon orbits are in different planes, with different values of i and Ω. The design procedure to deliver a suitable transfer between the planes also employs the 2BP-CR3BP patched model, given the advantage of initially exploring the problem analytically. First, the departure instant $\theta_{0_{Gan}}$, the initiating epoch for the transfer, is defined. Trajectories from the CR3BP that are departing Ganymede are converted to departure conics at the

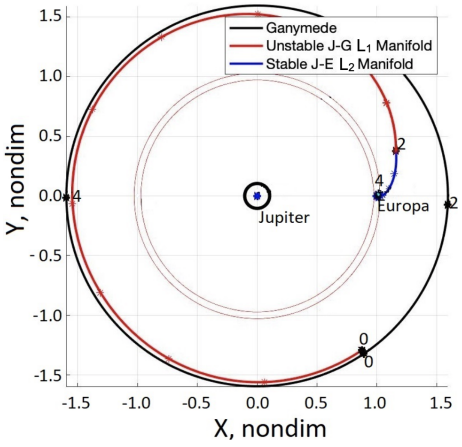

(a) Converged solution in the planar coupled spatial CR3BP represented in the Jupiter-Europa Rotating frame.

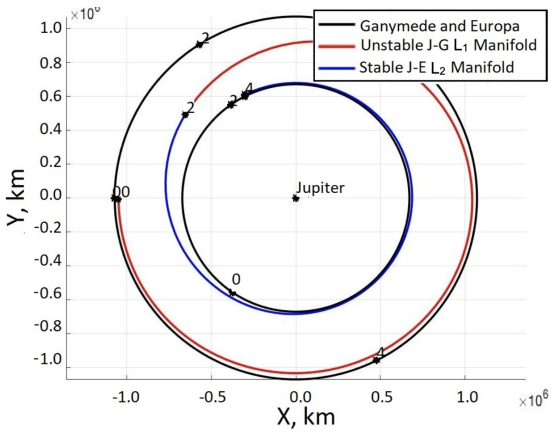

(b) Converged solution in the planar coupled spatial CR3BP represented in the Ecliptic J2000 Jupiter-centered inertial frame.

Figure 8. Converged solution in the planar coupled spatial CR3BP; Δv=0.9456 km/s and t_{tot}=9.47 days.

SoI (whose orbital elements depend upon $\theta_{0_{Gan}}$), and trajectories arriving in Europa's vicinity are transformed into back-propagated arrival conics at its SoI (whose orbital elements depend upon the arrival epoch, $\theta_{4_{Eur}}$). In this example, departure and arrival conics possess different values of Ω and i. The objective is the determination of the geometrical condition necessary for both departure and arrival conics to intersect, at some point in space, given a uniquely determined phase between the moons. The angle $\theta_{4_{Eur}}$ is assumed free since the arrival moon orbit is rephased such that an intersection between departure and arrival conics is accomplished. By applying spherical trigonometry[23] (Figure 9), it is possible to determine the angle of intersection for the departure and arrival conics with respect to their node line (right ascension of the ascending node), u_d and u_a repectively, between the two orbital planes for the moon orbits, given the difference in right ascension of the ascending nodes of the two conics, $\Delta\Omega = \Omega_d - \Omega_a$, and the inclinations of the two planes, i_d and i_a:

$$\begin{array}{ll} \sin(u_d) = \frac{\sin(i_a)\sin(\Delta\Omega)}{\sin(\psi)} & \cos(u_d) = \frac{\frac{\sin(i_a)\cos(\Delta\Omega)}{\cos(i_d)} - \cos(\psi)\tan(i_d)}{\sin(\psi)} \\ \sin(u_a) = \frac{\sin(i_d)\sin(\Delta\Omega)}{\sin(\psi)} & \cos(u_a) = \cos(\Delta\Omega)\cos(u_d) + \sin(\Delta\Omega)\sin(u_d)\cos(i_d) \end{array}, \tag{8}$$

where $\psi = \cos^{-1}(\cos(i_a)\cos(i_d) + \sin(i_a)\sin(i_d)\cos(\Delta\Omega))$. As a result, the true anomaly at which the departure conic intersects the plane is evaluated as $\theta_{d_{Intersection}}$ or $\theta_{d_{Intersection}} + \pi$, depending on the argument of periapsis for the departure conic, ω_d: $\theta_{d_{Intersection}} = u_d - \omega_d$. The spatial intersection of the departure conic occurs at:

$$r_{d_{Intersection}} = \frac{a_d(1-e_d^2)}{1 + e_d\cos(\theta_{d_{Intersection}} + n\pi)}, \text{ being } n = 0,\ 1. \tag{9}$$

For a successful spatial connection between the departure and arrival conic, the following relationship must hold for the arrival conic:

$$r_{d_{Intersection}} = \frac{a_a(1-e_a^2)}{1 + e_a\cos(\theta_{a_{Intersection}} + n\pi)}, \text{ being } n = 0,\ 1. \tag{10}$$

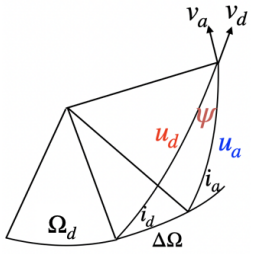

Figure 9. Intersection between two planes using spherical trigonometry.[23]

As a result, the true anomaly for the intersection of the arrival conic at $\theta_{a_{Intersection}}$ and $\theta_{a_{Intersection}} + \pi$ is obtained:

$$\cos(\theta_{a_{Intersection}} + n\pi) = \frac{\frac{p_a}{r_{d_{Intersection}}} - 1}{e_a}, \text{ being } n = 0,\ 1, \tag{11}$$

where $p_a = a_a(1 - e_a^2)$. From Eq. (11), given that $-1 \leq \cos(\theta_{a_{Intersection}} + n\pi) \leq 1$, a useful analytical condition is identified, one that must be fulfilled such that the arrival conic is rephased to directly intersect with the departure conic:

$$a_a(1 - e_a) \leq \frac{a_d(1 - e_d^2)}{1 + e_d cos(\theta_{d_{Intersection}} + n\pi)} \leq a_a(1 + e_a), \text{ being } n = 0,\ 1. \tag{12}$$

The angle $\theta_{d_{Intersection}}$ or $\theta_{d_{Intersection}} + \pi$ is generally defined by the i and Ω values for the departure and arrival planes as well as by ω_d, which depends on $\theta_{0_{Gan}}$. If the departure conic geometrical properties, given a value of $\theta_{0_{Gan}}$, meets the boundary conditions defined by the geometrical properties for the arrival conic, an intersection at $\theta_{d_{Intersection}}$, $\theta_{d_{Intersection}} + \pi$ or both $\theta_{d_{Intersection}}$ and $\theta_{d_{Intersection}} + \pi$ is possible. The lower boundary defines an arrival conic that is too small to connect with the departure conic; the upper limit represents an arrival conic that is too large to link with the departure conic. As a result, if the inequality constraint in Eq. (12) is fulfilled, the angle of intersection of the arrival conic $\theta_{a_{Intersection}}$ is obtained and, since the intersection occurs at $\theta_{a_{Intersection}}$ and $\theta_{a_{Intersection}} + \pi$, $\omega_a = u_a - \theta_{a_{Intersection}}$ is obtained and with it, the intersection point between the planes that leads to a smaller Δv is selected. The optimal phase for the arrival moon to yield such a configuration follows the same procedure as detailed for coplanar moon orbits.

Ganymede to Europa transfer. For purposes of comparison, the minimum Δv trajectory in the planar case is introduced for this application. First, the unstable manifold trajectory is propagated from the L_1 Lyapunov orbit in the J-G system towards the Ganymede SoI, where it evolves into a departure conic, similarly to the stable manifold trajectory that arrives at the L_2 Lyapunov orbit in the J-E system from the Europa SoI, where it is defined as an arrival conic. Given Eq. (12), it is possible to complete a feasibility analysis to locate a transfer between the two specified moons for a given departure angle from Ganymede $\theta_{0_{Gan}}$ (Figure 10). For every $\theta_{0_{Gan}}$, if the black line in Figures 10(a) and 10(b) is between the red and blue lines (lower and upper boundaries from Eq. (12), respectively), the total Δv, t_{tot}, and the position of Europa at the initial epoch $\theta_{0_{Eur}}$ are noted. Therefore, promising scenarios are available, such as the minimum Δv (Figure 11(a)) or minimum t_{tot} configurations (Figure 11(b)). These solutions are transferred to the coupled spatial CR3BP by using the necessary angles obtained in the 2BP-CR3BP patched spatial model: (a) measured from the ascending node line for the departing moon plane, the initial location of the moon where the trajectory starts and the intersection point between the planes (instant 0 and 2 in Figure 11, respectively); (b) measured from the ascending node line for the arrival moon plane, the initial location

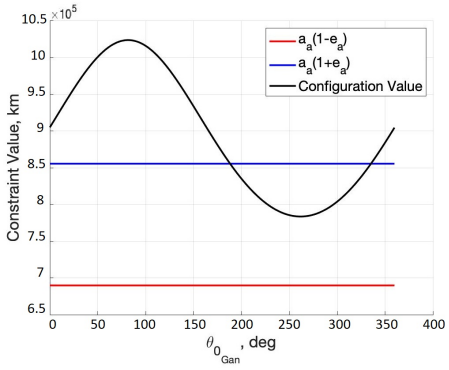

(a) Evaluation of the constraint Eq. (12).

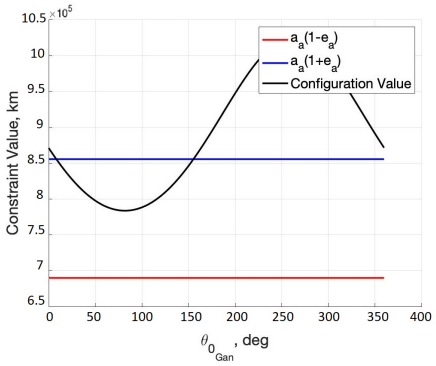

(b) Evaluation of the constraint Eq. (12).

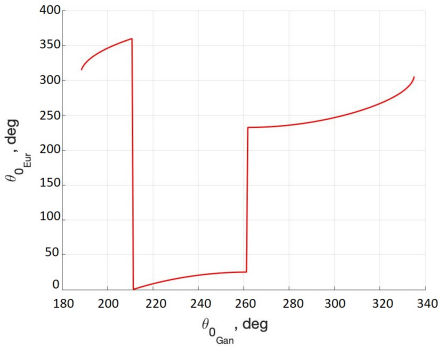

(c) Phase of Ganymede and Europa with respect to their ascending node direction at t_0.

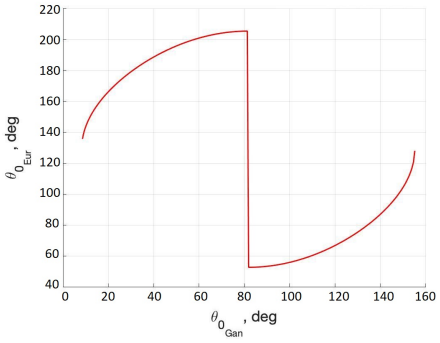

(d) Phase of Ganymede and Europa with respect to their ascending node direction at t_0.

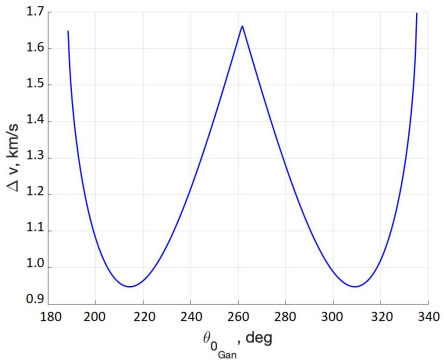

(e) Transfer Δv given a $\theta_{0_{Gan}}$.

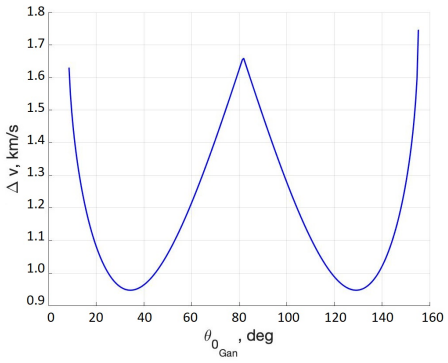

(f) Transfer Δv given a $\theta_{0_{Gan}}$.

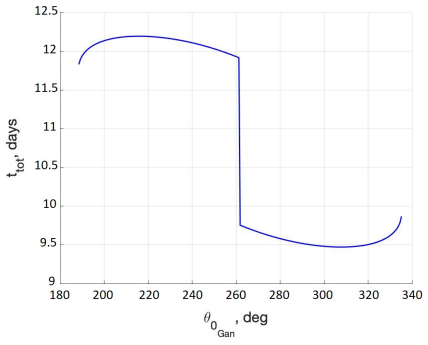

(g) Transfer t_{tot} given a $\theta_{0_{Gan}}$

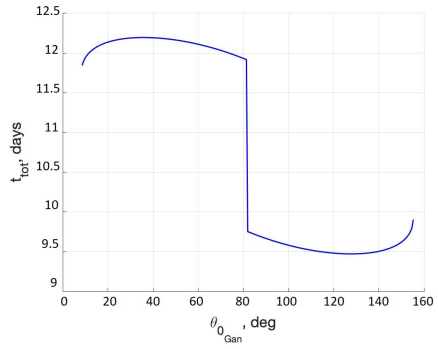

(h) Transfer t_{tot} given a $\theta_{0_{Gan}}$

Figure 10. Successful configurations with intersection at $\theta_{d_{Intersection}}$ (left column) and $\theta_{d_{Intersection}} + \pi$ (right column).

of the moon where the trajectory starts and the intersection point between the planes (instant 0 and 2 in Figure 11, respectively). To produce a continuous trajectory in the coupled spatial CR3BP, a multiple shooter serves as the basis for the differential corrections algorithm.[19] Given that departure trajectories are rotated onto the arrival moon plane, the problem is solved numerically by means of a central difference approximation. Both the minimum Δv and t_{tot} converged solutions in the coupled spatial CR3BP are thus produced (Figure 12).

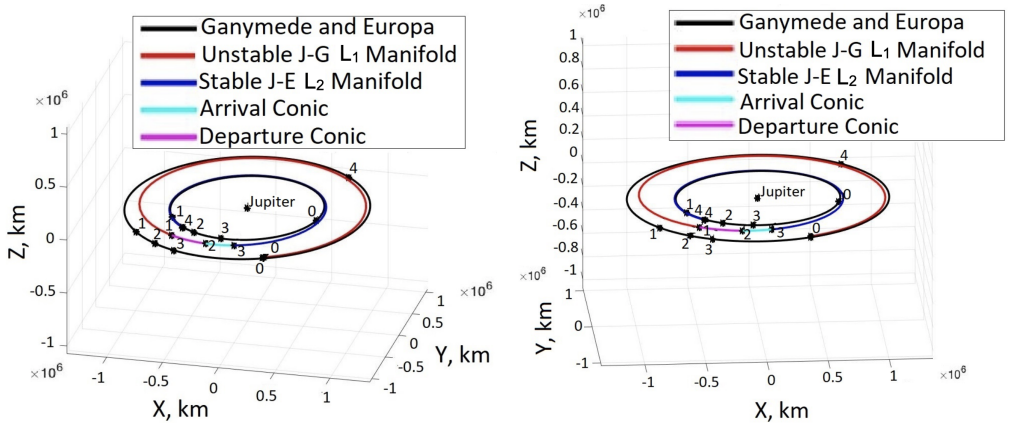

(a) Minimum Δv configuration. $\Delta v = 0.9448$ km/s and $t_{tot} = 9.473$ days.

(b) Minimum t_{tot} configuration. $\Delta v = 0.9455$ km/s and $t_{tot} = 9.471$ days.

Figure 11. Resulting transfer trajectory using the 2BP+CR3BP patched model (Ecliptic J2000 Jupiter-centered inertial frame).

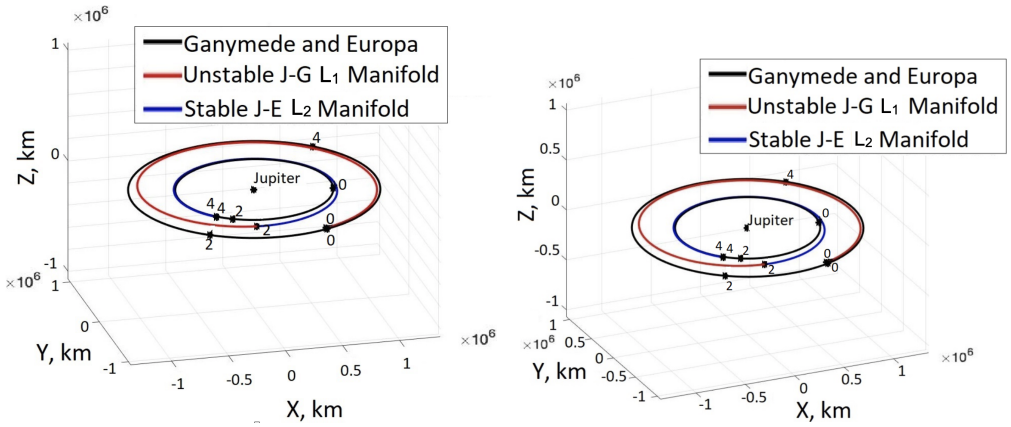

(a) Minimum Δv configuration. $\Delta v = 0.9422$ km/s and $t_{tot} = 9.473$ days.

(b) Minimum t_{tot} configuration. $\Delta v = 0.9428$ km/s and $t_{tot} = 9.472$ days.

Figure 12. Converged solution in the coupled spatial CR3BP (Ecliptic J2000 Jupiter-centered inertial frame).

Alternative for spatial cases. When the given configuration does not fulfill the condition in Eq. (12), yet the planar constraint represented by Eq. (6) is still satisfied, a successful transfer is guaranteed via two simple steps. First, the departure conic is propagated towards the intersection with the arrival plane and a Δv is applied to shift the conic to one with the same a_d and e_d, but in the plane

of the arrival moon. Then, the resulting conic tangentially intersects the arrival conic with the same Δv as if the transfer is accomplished assuming both moons are coplanar (Figure 13). Depending on mission requirements, one of the two strategies is selected (Figure 14). For this specific case, despite the fact that two Δvs lead to lower costs than a single Δv for most initial epochs (i.e., $\theta_{0_{Gan}}$), such a behavior might not hold for other transfers or systems. Note that for this alternative, the subscript "5" denotes the arrival instant due to the fact that another arc is incorporated.

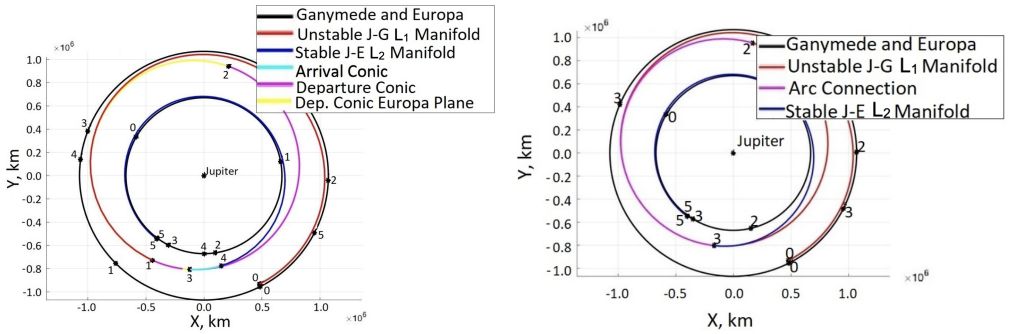

(a) Departure to intermediate conic (yellow), and tangential connection to arrival conic. $\Delta v_{tot} = 1.0023$ km/s and $t_{tot} = 15.02$ days. 2BP-CR3BP Patched Model.

(b) Transfer from departure arc to intermediate arc, and connect tangentially to arrival arc. $\Delta v_{tot} = 1.0101$ km/s and $t_{tot} = 15.02$ days. Coupled spatial CR3BP.

Figure 13. Strategy to guarantee a transfer when Eq. (12) fails, but Eq. (6) is fulfilled. Both figures are represented in the Ecliptic J2000 Jupiter centered inertial frame.

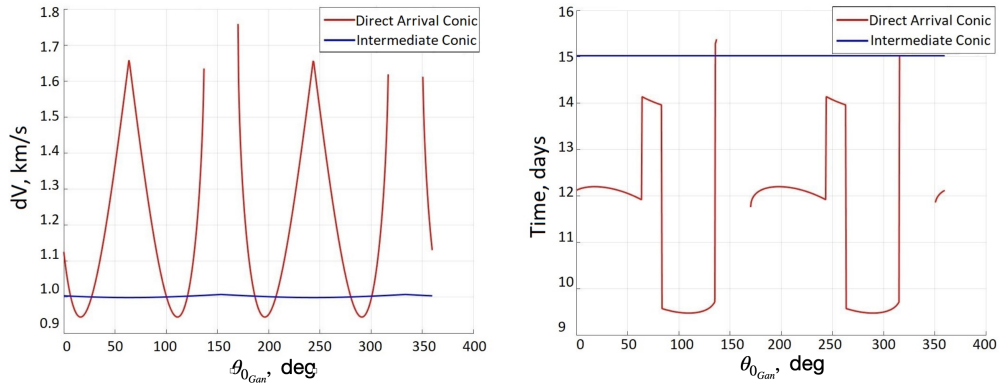

(a) Total Δv depending on $\theta_{0_{Gan}}$.

(b) Final t_{tot} depending on $\theta_{0_{Gan}}$.

Figure 14. Total Δv and t_{tot} for two strategies: directly from departure to arrival conic (Direct Arrival Conic); from departure to an intermediate conic in the arrival plane with tangential connection to arrival conic (Intermediate Conic).

Comparison between transfers for coplanar and non-coplanar moon orbits

It is possible to compare results between the solutions produced assuming coplanar and non-coplanar moon orbits. This comparison is accomplished within the context of the example previously introduced: a transfer from a Lyapunov orbit in the vicinity of L_1 in the Jupiter-Ganymede

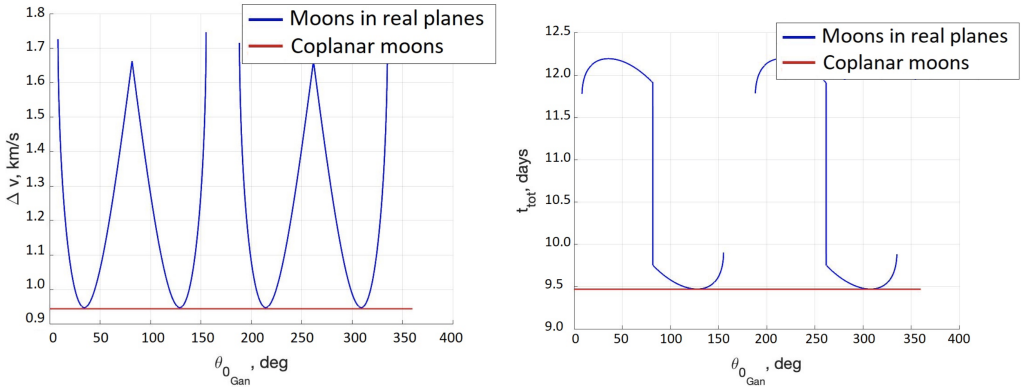

(a) Total Δv depending on $\theta_{0_{Gan}}$ for both assuming moons are coplanar and in their real planes.

(b) Final t_{tot} depending on $\theta_{0_{Gan}}$ for both assuming moons are coplanar and in their real planes.

Figure 15. Comparison of the total Δv and t_{tot} for both assuming moons are coplanar and in their real planes. In the case of moons being in their real planes, successful configurations with intersection at $\theta_{d_{Intersection}}$ and $\theta_{d_{Intersection}} + \pi$ are included in the same plot for the sake of comparison.

system towards an L_2 Lyapunov orbit in the Jupiter-Europa system via unstable and stable manifolds. If the transfer design approach assumes both moon orbits are coplanar, Figure 15 illustrates that the total Δv of the transfer as well as t_{tot} remains constant regardless of the initial epoch $\theta_{0_{Gan}}$. Nevertheless, when the moons are incorporated in their true orbital planes, despite the fact that their relative inclinations are small, and given that there is a difference between Ω_G and Ω_E , it is apparent in Figure 15(a) that, depending on $\theta_{0_{Gan}}$, the single Δv varies from a minimum value similar to that obtained in the planar case to a maximum value of 1.75 km/s. Similarly, t_{tot} varies from a value in the planar case to nearly 12.25 days depending on $\theta_{0_{Gan}}$ (Figure 15(b)).

There exist some departure angles, $\theta_{0_{Gan}}$, where a connection between the departure and arrival trajectories does not occur, due to the fact that Eq. (12) is not satisfied. Generally, this work reflects that the Δv and t_{tot} obtained assuming the moon orbits are coplanar are undervalued with respect to the spatial model, since the results sensibly vary depending on the position of Ganymede at its plane at departure (Figure 15). Although the coplanar analysis supplies preliminary information concerning the transfers between the moons, this spatial technique supplies more accurate information to exploit in real applications assuming a goal for a direct transfer. For a transfer involving a single maneuver, the cost and time of a transfer between two moons are entirely dependent upon the initial epoch, represented in this example with $\theta_{0_{Gan}}$, with some angles providing no access whatsoever.

A SPATIAL APPLICATION BETWEEN TITANIA AND OBERON

Consider a s/c located in an L_2 northern halo orbit in the Uranus-Titania (U-T) system with a given Jacobi Constant value $JC_d = 3.0035$, and assume that the target location is an L_1 southern halo orbit ($JC_a = 3.003$) in the Uranus-Oberon (U-O) system (see Table 2 for system data). Unstable manifolds depart from the L_2 halo orbit in the U-T system and, similarly, stable manifolds arrive into the L_1 halo orbit in the U-O system. As illustrated in Figure 16, the unstable manifold trajectories are propagated from the L_2 northern halo orbit in the U-T system towards the Titania SoI, where they are evaluated as departure conics. The stable manifold trajectories associated with the L_1 southern halo orbit in the U-O system, reach the Oberon SoI in backwards time, where the states are transformed to arrival conics. Numerical algorithms to produce feasible transfers between spatial

orbits assuming coplanar moons are detailed by other authors.[10] In this investigation, the spatial strategy assumes that the moons are modeled in their respective true orbital planes and, thus, the spatial transfer is derived directly. A desired unstable manifold trajectory and a stable manifold trajectory that lead to spatial conics that fulfill Eq. (12) are selected, and the 2BP-CR3BP patched model is used to deliver a useful initial guess to pass to the coupled spatial CR3BP.

Table 2. Orbital data of Titania and Oberon (SPICE,[20] last accessed 08/05/2020).

	Semi-Major Axis [km]	Orbital Period [day]	μ $[10^{-5}]$	e	Inclination measured from Ecliptic J2000 [degree]	Right Ascension of the Ascending Node [degree]
Titania	$4.363 \cdot 10^5$	8.708	3.91675	0.00187	97.829	167.627
Oberon	$5.836 \cdot 10^5$	13.471	3.54363	0.00117	97.853	167.720

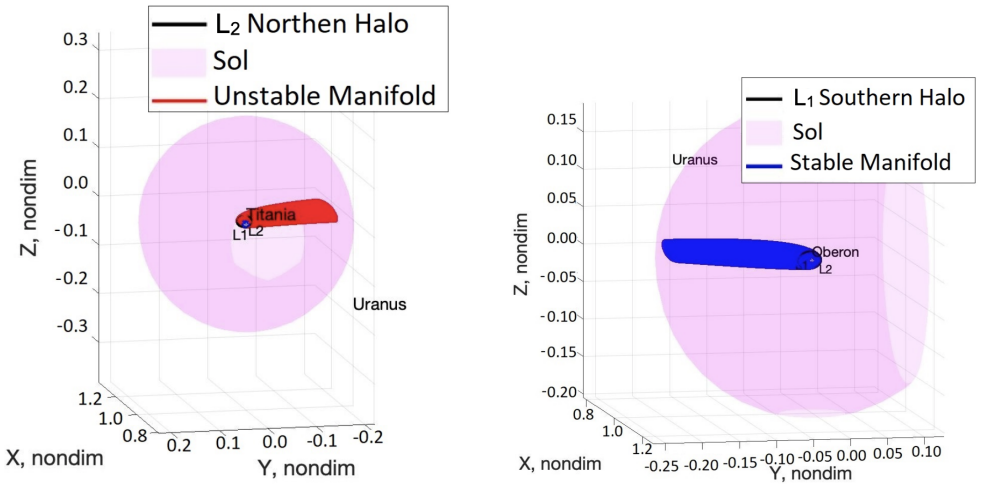

(a) Unstable manifolds propagated from L_2 halo orbit with a $JC_d = 3.0035$ towards Titania SoI in the U-T rotating frame.

(b) Stable manifolds propagated towards L_1 halo orbit with a $JC_a = 3.003$ from Oberon SoI in the U-O rotating frame.

Figure 16. Departure manifolds from the Titania vicinity (left) and arrival manifolds to the local Oberon region (right).

Given Eq. (12), it is possible to directly observe potential intersections between both manifold trajectories given an initial departure angle from Titania with respect to its ascending node, $\theta_{0_{Tit}}$. If the configuration is within the limits of such a constraint, a successful transfer occurs given an ideal rephasing of the arrival at Oberon with respect to its ascending node, $\theta_{4_{Obe}}$. Nevertheless, observe in Figure 17 that, since the stable manifold trajectory is spatial when it crosses Oberon's SoI, Ω_a and i_a vary depending on the arrival angle, $\theta_{4_{Obe}}$; of course, these are different from the values for the Oberon orbit, Ω_O and i_O. Therefore, when the rephasing technique is applied using Eq. (7), the angle σ is defined in the plane of the conic and not in the plane of the arrival moon. Thus, the departure and arrival conics no longer intersect. However, if Eq. (12) is fulfilled, an ideal rephasing for such a transfer to occur does exist given a $\theta_{0_{Tit}}$. Therefore, σ is projected onto the plane of the arrival moon, offering a sufficiently close initial guess to encounter the intersection using a differential corrections scheme. Since $\theta_{0_{Tit}}$ is fixed, the conic state departing the SoI is also fixed, but not the propagation time at which it intersects the arrival conic, t_d. Then, an initial guess for

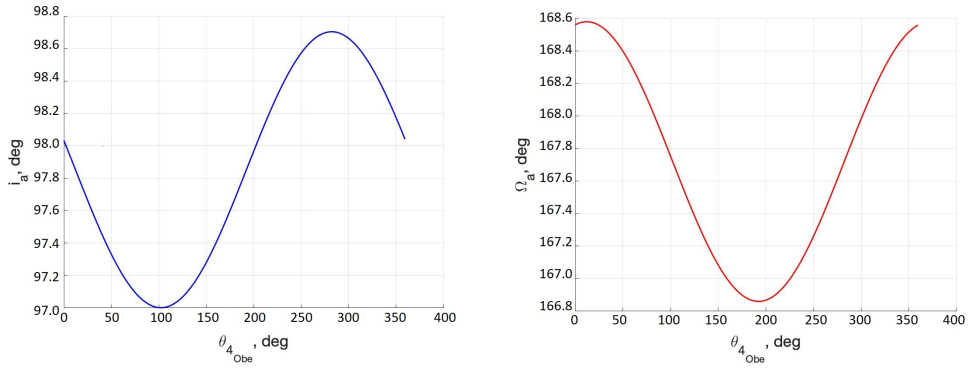

(a) i_a evolution with respect to $\theta_{4_{Obe}}$.

(b) Ω_a evolution with respect to $\theta_{4_{Obe}}$.

Figure 17. Evolution of Ω_a and i_a depending on the arrival angle at Oberon.

the angle $\theta_{4_{Obe}}$ is constructed using the projected σ into Eq. (7). The arrival trajectory into the L_1 southern halo orbit in the U-O system is back-propagated towards the SoI of Oberon in the CR3BP, leading to an arrival conic whose Ω_a and i_a depend upon $\theta_{4_{Obe}}$. The propagation time at which the arrival conic intersects the departure conic, t_a, is considered free. As a result, the objective is the determination of a design variable vector, $\bar{X}$, defined by $\theta_{4_{Obe}}$, t_d and t_a, that satisfies the constraint vector, $\bar{F}(\bar{X}) = \bar{0}$, and ensures position continuity at the intersection between the departure and arrival conic:

$$\bar{F} = \left\{ \begin{array}{c} x_d - x_a \\ y_d - y_a \\ z_d - z_a \end{array} \right\} = \bar{0}, \; \bar{X} = \left\{ \begin{array}{c} \theta_{4_{Obe}} \\ t_d \\ t_a \end{array} \right\}. \tag{13}$$

To solve for $\bar{X}$, a Taylor series (truncated to first order) is expanded on $\bar{F}(\bar{X}) = \bar{0}$ about the free-variable initial guess, $\bar{X}_0$: $\bar{F}(\bar{X}_0) + \mathbf{DF}(\bar{X}_0)(\bar{X} - \bar{X}_0) = \bar{0}$. The vector $\bar{X}_0$ is defined with the values $\theta_{4_{Obe}}$, t_d and t_a obtained from the projection of σ onto the arrival moon plane. The matrix $\mathbf{DF}$ is numerically computed:

$$\mathbf{DF} = \left[\begin{array}{ccc} \frac{\partial(x_d - x_a)}{\partial \theta_{4_{Obe}}} & \frac{\partial(x_d - x_a)}{\partial t_d} & \frac{\partial(x_d - x_a)}{\partial t_a} \\ \frac{\partial(y_d - y_a)}{\partial \theta_{4_{Obe}}} & \frac{\partial(y_d - y_a)}{\partial t_d} & \frac{\partial(y_d - y_a)}{\partial t_a} \\ \frac{\partial(z_d - z_a)}{\partial \theta_{4_{Obe}}} & \frac{\partial(z_d - z_a)}{\partial t_d} & \frac{\partial(z_d - z_a)}{\partial t_a} \end{array} \right], \tag{14}$$

and, since **DF** is square and can be inverted, the problem is solved using a Newton approach. Given the sufficiently close initial guess, a converged solution is delivered in only a few iterations. As a result, for every $\theta_{0_{Tit}}$, a similar feasibility analysis to that appearing in Figure 10 is produced. Promising scenarios are, thus, available for direct transfers, such as a minimum-Δv configuration (Figure 18), which is transferred to the coupled spatial CR3BP (Figure 19) by means of solving the problem using a differential corrections algorithm.[19]

DISCUSSION AND CONCLUDING REMARKS

Trajectory design for transfers between different moons moving in the vicinity of a common planet is a balance between diverse constraints, priorities and requirements to enable successful missions. In this investigation, a method to determine transfers between two different moons moving around a common planet is presented within the context of the CR3BP. The analysis supports

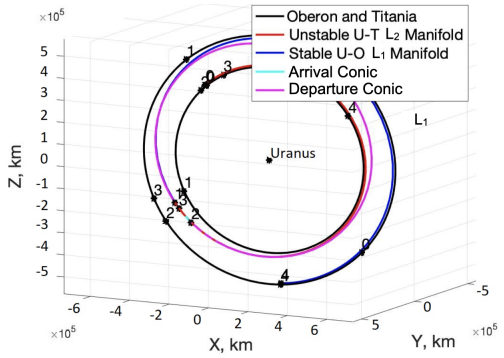

Figure 18. Transfer from northern halo L_2 in the Uranus-Titania system to southern halo L_1 in the Uranus-Oberon system. (Ecliptic J2000 Uranus centered inertial frame). $\Delta v_{tot} = 62.6$ m/s and $t_{tot} = 28.5$ days. 2BP-CR3BP patched model.

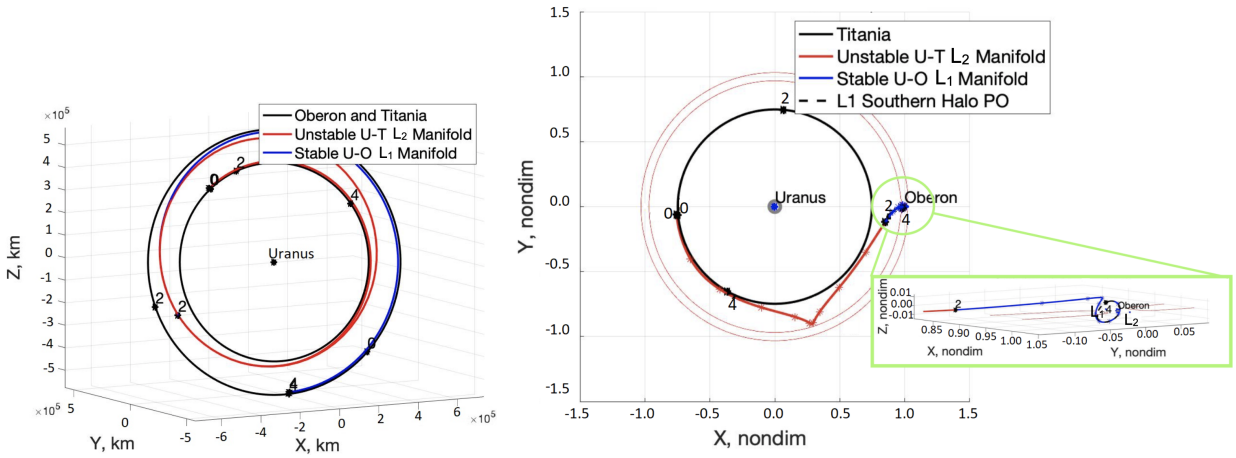

(a) Transfer between L_2 northern halo orbit of Uranus-Titania system, to L_1 southern halo orbit of Uranus-Oberon system in the Ecliptic J2000 Uranus centered inertial frame.

(b) Transfer between an L_2 northern halo orbit of Uranus-Titania system, to L_2 southern halo orbit of Uranus-Oberon system in the Uranus-Oberon rotating frame.

Figure 19. Converged solution in the coupled spatial CR3BP for a transfer between an L_2 northern halo orbit of Uranus-Titania system, to L_1 southern halo orbit of Uranus-Oberon system $\Delta v = 45.7$ m/s and $t_{tot} = 28.44$ days.

transfers between libration point orbits near different moons. Structures that stem from the CR3BP formulation are smoothly incorporated for moon tour design by blending conics from the 2BP with arcs from the CR3BP. In particular, transfers between planar and spatial libration point orbits of two different planet-moon systems are accomplished. The main advantage of this approach is that it does not rely on the assumption that the moon orbits are coplanar, thus, determining direct solutions with the moons in their true orbital planes. By means of incorporation of the 2BP-CR3BP patched model, two analytical constraints are identified for both coplanar and non-coplanar moon orbits. These analytical conditions determine the geometrical relationships between the conics and the orbital planes such that the epoch of the arrival moon is shifted for an intersection to occur. Given the small eccentricities of the moon orbits and that moons are located in their true orbital planes at a certain epoch, the method yields phasing of the moons that is consistent with the real moon orbits. As a result, these analytical expressions are leveraged to ease the design process and yield successful transfers between CR3BP arcs in the coupled spatial CR3BP, where analytical solutions are difficult.

The tour design process is validated in two different multi-moon systems: transfers from Ganymede to Europa as well as from Titania to Oberon are encountered. Both systems present entirely different moon orbital plane properties. As long as the spatial constraints are fulfilled, it is possible to produce a transfer solution between planar and spatial CR3BP arcs connecting two moons. This fact is also reflected in Figure 20(b), where a transfer between two moons with the same properties as Ganymede and Europa in Table 1 but located in very different planes is obtained. Given the purely mathematical properties of the constraints, moon-to-moon transfers between CR3BP arcs are designed both for outward and inward journeys (see also Figure 20(a) for an Europa to Ganymede example). Note that the focus of this investigation is direct transfers from one moon to another; using an intermediate conic remains an option that is likely less costly depending on the problem.

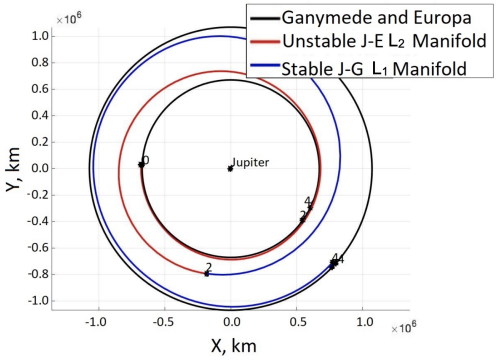

(a) Minimum Δv configuration in the spatial coupled CR3BP, from Europa to Ganymede. $\Delta v = 0.94$ km/s and $t_{tot} = 12.197$ days.

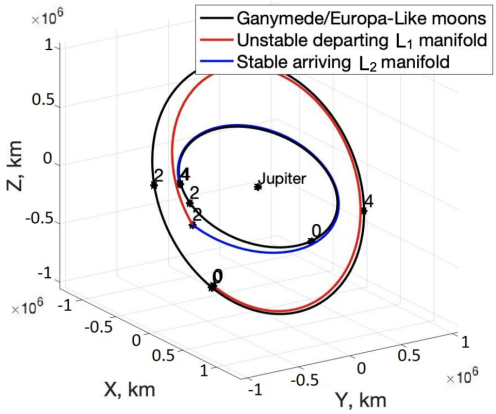

(b) Minimum Δv configuration in the spatial coupled CR3BP, considering $\Omega_{JG} = 100°$, $i_{JG} = 60°$, $\Omega_{JE} = 200°$ and $i_{JG} = 20°$. $\Delta v = 12.98$ km/s and $t_{tot} = 11.83$ days. This figure is uniquely presented to justify the validity of the method.

Figure 20. Converged solutions in the spatial coupled CR3BP for other examples.

In conclusion, all the necessary steps are provided to produce a direct transfer between two distinct moons in their true orbital planes in the coupled spatial CR3BP. For any given angle of departure from one moon, if Eq. (12) is fulfilled, a unique natural transfer between CR3BP arcs is obtained with a single Δv, given that the unique natural configuration between moons in their respective planes is acquired for that given scenario. Therefore, for every departure angle, as long as the configuration is between the limits in Eq. (12), the total Δv, t_{tot}, and the phase of the arrival moon at departure are noted. Furthermore, by means of an analytical exploration of the problem, the method provides the phase combinations between the moons that yield the most cost-efficient results. Since the resulting spatial transfer is ultimately designed within the context of the coupled spatial CR3BP, it may be more effective in transitioning to a higher-fidelity ephemeris model. Note that the constraint in Eq. (12) is significant for designing trajectories not only in the coupled spatial CR3BP, but also in the fundamental CR3BP when the motion is governed by the larger primary.

ACKNOWLEDGEMENTS

Assistance from colleagues in the Multi-Body Dynamics Research group at Purdue University is appreciated as is the support from the Purdue University School of Aeronautics and Astronautics and

College of Engineering including access to the Rune and Barbara Eliasen Visualization Laboratory.

REFERENCES

[1] R. Diehl, D. Kaplan, and P. Penzo, *Satellite tour design for the Galileo mission*. AIAA, 21st Aerospace Sciences Meeting, 1983, 10.2514/6.1983-101.

[2] N. Strange, T. Goodson, and Y. Hahn, *Cassini Tour Redesign for the Huygens Mission*. AIAA/AAS Astrodynamics Specialist Conference and Exhibit, 2002, 10.2514/6.2002-4720.

[3] S. Plaut, S. Barabash, L. Bruzzone, M. Dougherty, C. Erd, L. Fletcher, G. Gladstone, O. Grasset, L. Gurvits, P. Hartogh, H. Hussmann, L. Iess, R. Jaumann, Y. Langevin, P. Palumbo, G. Piccioni, D. Titov, and J.-E. Wahlund, "Jupiter Icy Moons Explorer (JUICE): Science Objectives, Mission and Instruments," *Lunar and Planetary Science Conference*, Vol. 45, 01 2014.

[4] C. B. Phillips and R. T. Pappalardo, "Europa Clipper Mission Concept: Exploring Jupiter's Ocean Moon," *Eos, Transactions American Geophysical Union*, Vol. 95, No. 20, 2014, pp. 165–167, 10.1002/2014EO200002.

[5] R. Lorenz, E. Turtle, J. Barnes, M. Trainer, D. Adams, K. Hibbard, C. Sheldon, K. Zacny, P. Peplowski, D. Lawrence, M. Ravine, T. McGee, K. Sotzen, S. MacKenzie, J. Langelaan, S. Schmitz, L. Wolfarth, and P. Bedini, "Dragonfly: A rotorcraft lander concept for scientific exploration at titan," *Johns Hopkins APL Technical Digest (Applied Physics Laboratory)*, Vol. 34, 10 2018, pp. 374–387.

[6] W. Koon, M. Lo, J. Marsden, and S. Ross, *Constructing a Low Energy Transfer Between Jovian Moons*, Vol. 292, pp. 129–145. 01 2001, 10.1090/conm/292/04919.

[7] M. Kakoi, K. Howell, and D. Folta, "Access to Mars from Earth–Moon libration point orbits: Manifold and direct options," *Acta Astronautica*, Vol. 102, 10 2014, 10.1016/j.actaastro.2014.06.010.

[8] C. R. Short, D. Blazevski, K. C. Howell, and G. Haller, "Stretching in phase space and applications in general nonautonomous multi-body problems," *Celestial Mechanics and Dynamical Astronomy*, Vol. 122, No. 3, 2015, pp. 213–238, 10.1007/s10569-015-9617-4.

[9] E. Fantino and R. Castelli, "Efficient design of direct low-energy transfers in multi-moon systems," *Celestial Mechanics and Dynamical Astronomy*, Vol. 127, 10 2016, 10.1007/s10569-016-9733-9.

[10] E. Fantino, R. M. Flores, and A. N. Al-Khateeb, "Efficient Two-Body Approximations of Impulsive Transfers between Halo Orbits," *69th International Astronautical Congress (IAC), Bremen, Germany*, 2018.

[11] E. Fantino, F. Salazar, and E. M. Alessi, "Design and performance of low-energy orbits for the exploration of Enceladus," February 2020.

[12] F. Topputo, M. Vasile, and F. Bernelli-Zazzera, "Low Energy Interplanetary Transfers Exploiting Invariant Manifolds of the Restricted Three-Body Problem," *Journal of the Astronautical Sciences*, Vol. 53, 10 2005, pp. 353–372.

[13] G. Colasurdo, A. Zavoli, A. Longo, L. Casalino, and F. Simeoni, "Tour of Jupiter Galilean moons: Winning solution of GTOC6," *Acta Astronautica*, Vol. 102, 2014, pp. 190 – 199, https://doi.org/10.1016/j.actaastro.2014.06.003.

[14] A. E. Lynam, K. W. Kloster, and J. M. Longuski, "Multiple-satellite-aided capture trajectories at Jupiter using the Laplace resonance," *Celestial Mechanics and Dynamical Astronomy*, Vol. 109, No. 1, 2011, pp. 59–84, 10.1007/s10569-010-9307-1.

[15] S. Campagnola, P. Skerritt, and R. P. Russell, "Flybys in the planar, circular, restricted, three-body problem," *Celestial Mechanics and Dynamical Astronomy*, Vol. 113, No. 3, 2012, pp. 343–368, 10.1007/s10569-012-9427-x.

[16] P. Grover and S. Ross, "Designing Trajectories in a Planet–Moon Environment Using the Controlled Keplerian Map," *Journal of Guidance, Control, and Dynamics*, Vol. 32, 03 2009, pp. 437–444, 10.2514/1.38320.

[17] G. Lantoine, R. P. Russell, and S. Campagnola, "Optimization of low-energy resonant hopping transfers between planetary moons," *Acta Astronautica*, Vol. 68, No. 7, 2011, pp. 1361 – 1378, https://doi.org/10.1016/j.actaastro.2010.09.021.

[18] V. Szebehely, *The Restricted Problem*. Vienna: Springer Vienna, 1974.

[19] A. Haapala and K. Howell, "A Framework for Constructing Transfers Linking Periodic Libration Point Orbits in the Spatial Circular Restricted Three-Body Problem," *International Journal of Bifurcation and Chaos*, Vol. 26, 05 2015, p. 1630013, 10.1142/S0218127416300135.

[20] C. Acton, N. Bachman, B. Semenov, and E. Wright, "A look toward the future in the handling of space science mission geometry," *Planetary and Space Science*, 2017.

[21] W. L.-S. WEN, "A Study of Cotangential, Elliptical Transfer Orbits in Space Flight," *Journal of the Aerospace Sciences*, Vol. 28, No. 5, 1961, pp. 411–417, 10.2514/8.9010.

[22] A. Viale, "Low-energy tour of the Galilean moons," Master's thesis, Università degli Studi di Padova, 2015/2016.

[23] D. A. Vallado, *Fundamentals of astrodynamics and applications, Space Technology Series*. McGraw-Hill, New York, 1997.